International Journal of Offshore and Polar Engineering
Vol. 7, No. 4, December 1997 (ISSN 1053-5381)

Analytical Approximation for the Dynamic Bending Moment at the Touchdown Point of a Catenary Riser

J.A.P. Aranha
Department of Naval Architecture and Ocean Engineering

C.A. Martins* and C.P. Pesce*
Department of Mechanical Engineering
Escola Politécnica, University of São Paulo, São Paulo, Brazil

ABSTRACT

This paper introduces an analytical approximation, of a boundary layer type, for the dynamic bending moment at the touchdown point of a catenary riser. The approximation is based on a quasi-linear frequency domain solution of a cable ($EJ = 0$), the only source of nonlinearity being the viscous drag on the riser, and it takes care of the motion of the touchdown point, a specially important phenomenon in the fatigue analysis. In spite of the fact that this motion is predicted from a quasi-linear frequency domain model, the final expression for the moment is strongly nonlinear and compares very well, for the low sea states used in the fatigue analysis, with results obtained from nonlinear time domain simulation; as a matter of fact, even for the extreme sea condition in Campos Basin the comparison between the analytical approximation and numerical results is reasonable. The expression for the moment depends nonlinearly, although in an explicit way, on two quasi-linear dynamic variables of the cable: the displacement $x_0(t)$ of the touchdown point and the dynamic tension $\tau(t)$. In this way, the obtained expression can also become useful in the study of the complex nonlinear statistical behavior of the riser's bending moment in the vicinity of the touchdown point.

INTRODUCTION

The oil industry has lately become interested in the study of the technical feasibility of a steel catenary riser anchored in a deep-water floating production system (Phifer et al., 1994). Besides some aspects related to their installation, the troublesome spots of the steel catenary riser are located at the suspended end, where a flexible joint has to be used, and at the touchdown point, where the bending moment, both static and dynamic, must be evaluated.

The problem is essentially nonlinear, the main sources of nonlinearity being the fluid drag along the suspended length and the unilateral contact force between the soil and riser in the touchdown region. Thus, several commercial computer programs, developed to analyze this problem, use time domain simulation, a procedure that is complicated by the existence of discrepant time and length scales in the problem. In fact, besides the "large" time and length scales of the catenary, one must deal with a "short" time scale, related with the axial elastic stretching, and with a "short" length scale, due to the bending stiffness effect near the touchdown point and the flexible joint.

If discrepancies in scales cause, in general, numerical difficulties in time domain simulation, they make it easier to derive asymptotic approximations. In this paper, a quasi-linear frequency domain solution of a cable (bending stiffness $EJ = 0$) is used to develop an approximation, of a boundary layer type, for the dynamic moment at the touchdown point of a steel catenary riser. The only source of nonlinearity in the cable's ($EJ = 0$) dynamic solution is the fluid drag, which is dealt with in a standard way, namely, by using an equivalent linear damping based on the equality of the dissipated power and an iterative technique to obtain the final response.

The analytical expression for the bending moment takes care of the horizontal motion of the touchdown point, an essential aspect in the fatigue analysis of the riser. As will be seen along the paper, the bending moment in the touchdown region depends, in a strong nonlinear way, on only two quasi-linear dynamic variables of the cable ($EJ = 0$): the displacement $x_0(t)$ of the touchdown point and the dynamic tension $\tau(t)$.

The comparison between the analytical results here derived with the numerical results obtained from nonlinear time domain models shows a very good agreement for the low sea states used in the fatigue analysis; as a matter of fact, the comparison is reasonable even for the extreme sea state in Campos Basin if the riser is assumed to be anchored in a semisubmersible platform.

This work reviews the basic geometric definitions, discusses some features of the static catenary solution and introduces a local bending stiffness correction in the vicinity of the touchdown point. In addition, the dynamic problem is analyzed and the analytical approximation for the dynamic moment at the touchdown is derived. Finally, some numerical results, displaying the agreement between the analytical approximation and nonlinear time domain models are presented.

BASIC DEFINITIONS AND STATIC SOLUTION

One considers here the geometric configuration of a cable ($EJ = 0$) with a weight q per unit of length, suspended at sea level by a tension T_B and subjected also to an ocean current $V(z)$. The cable touches the ground at point O, supposed to be the origin of the Cartesian system (x,z), with the z axis being vertical and pointing upwards. The water depth is h, the suspended length of the cable is l, and the cable is assumed anchored at point A on the ground, distant l_G from O; the total length of the cable is $l + l_G$. If s is the curvilinear coordinate along the suspended length, with $s = 0$ at O,

*ISOPE Member.

Received September 4, 1996: revised manuscript received by the editors July 3, 1997. The original version was presented directly to the Journal on September 4, 1996.
KEY WORDS: Catenary riser, dynamic bending moment, touchdown point, analytical approximation.

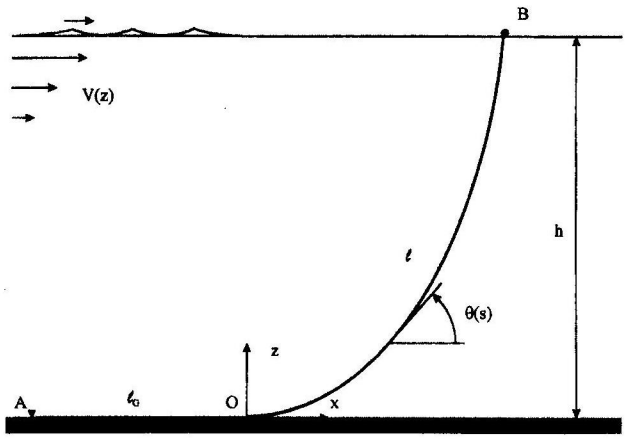

Fig. 1 Static configuration and some geometric definitions

and $\theta(s)$ is the angle between the cable's tangent and the horizontal, the geometry of the cable is defined by the pair of functions $(x(s); z(s))$ while its static equilibrium is characterized by the tension $T(s)$, with $T(l) = T_B$ and $T(0) = T_0$. Throughout this work the problem is assumed to be two-dimensional, in the plane (x,z), and the friction coefficient between the riser and the soil is denoted by μ.

As will be seen a bit later, the flexural stiffness of the riser affects weakly the geometry of the cable (catenary); if EJ is this stiffness, one has, in first approximation:

$$M(s) = EJ\frac{d\theta}{ds}(s) \tag{1a}$$

while at the touchdown:

$$M_0 = M(0) = EJ\frac{q}{T_0} \tag{1b}$$

the above expression being always exact for a catenary, the effect of the ocean current influencing it indirectly through T_0.

The curvature of the catenary is discontinuous at the touchdown point: It is equal to q/T_0 at the right of this point and to zero at the left. The effect of the flexural stiffness EJ is to smooth the transition between these two values of the curvature while displacing to the left the actual position of the touchdown point. If $z = Z_{f,0}(x)$ defines the geometric equilibrium configuration in the vicinity of O. influenced by the bending stiffness, the equilibrium is locally determined by the equation:

$$EJ\frac{d^4Z_{f,0}}{dx^4} - T_0\frac{d^2Z_{f,0}}{dx^2} = -q \tag{2a}$$

since $\theta(s) << 1$ and so $x \cong s$.

The "flexural length" λ, defined by the expression:

$$\lambda = \sqrt{\frac{EJ}{T_0}} \tag{2b}$$

gauges the geometric scale where the flexural stiffness is relevant; typically $\lambda \cong 10$ m and it is much smaller than the suspended length l. The moment is given by the relation $M_{f,0}(x) = EJ\, d^2Z_{f,0}/dx^2$ and the general solution of Eq. 2a can be written as:

$$M_{f,0}(x) = M_0 + C_1 e^{-(x-x_f)/\lambda} + C_2 e^{+(x-x_f)/\lambda}$$

$$EJ\frac{dZ_{f,0}}{dx} = M_0 x - \lambda C_1 e^{-(x-x_f)/\lambda} + \lambda C_2 e^{+(x-x_f)/\lambda} + C_3$$

where C_1, C_2, C_3 are constants of integration and x_f is the position of the touchdown point when the flexural stiffness is incorporated. When $x/\lambda >> 1$ one must have $M_{f,0}(x) \to M_0$ and $EJdZ_{f,0}/dx \to M_0 x$, since the solution of Eq. 2a must approach the catenary solution in this limit; it follows then that $C_2 = C_3 = 0$. At the touchdown point $x = x_f$ the conditions $M_{f,0}(x_f) = dZ_{f,0}/dx(x_f) = 0$ must be fulfilled, and so $C_1 = -M_0$; $x_f = -\lambda$. The touchdown point is displaced λ to the left and the actual moment is given by ($s \cong x$):

$$M_{f,0}(s) = \frac{1}{2}(1+sign(s+\lambda))\left[1-e^{-(s+\lambda)/\lambda}\right]M_0 \tag{2c}$$

These results will be used below.

DYNAMIC RESPONSE IN VICINITY OF TOUCHDOWN POINT

The riser is dynamically excited by the imposed motion at point B, anchored on the floating system, and by the direct action of the wave along its suspended length. In the major part of this section one considers the dynamic response of a cable ($EJ = 0$), ignoring the influence of the bending stiffness; in the last item this effect will be locally incorporated, as was done in the static analysis presented above.

Boundary Condition at Dynamic Touchdown Point

As discussed above, the static touchdown point of the cable ($EJ = 0$) is assumed to be at origin O of the coordinate system (x,z); if $z = Z_0(x)$ defines the cable's static configuration in the vicinity of O, the following boundary conditions are satisfied at this point:

$$Z_0(0) = 0 \tag{3a}$$

$$\frac{dZ_0}{dx}(0) = 0 \tag{3b}$$

As will be seen below, a similar boundary condition must be enforced at the *instantaneous* position of the touchdown point, when the horizontal velocity of this point is smaller than the "cable" wave velocity in the region, defined by the expression:

$$c_0 = \sqrt{\frac{T_0}{(m+m_a)}} \tag{4}$$

with m being the riser's mass per unit of length and m_a the added mass.

The derivation of this result, due to Triantafyllou et al. (1985) and based on a work by Burridge et al. (1982), is summarized next. In fact, if $z = Z(x,t)$ defines the dynamic configuration in the vicinity of O and $x = x_0(t)$ is the instantaneous position of the touchdown point, then:

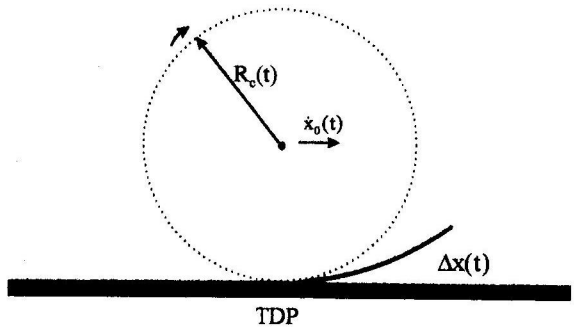

Fig. 2 Dynamic equilibrium of a piece of riser of length $\Delta x(t)$ and circular cylinder, rolling without slipping together with riser

$$Z(x_0(t),t) = 0 . \tag{5a}$$

The total derivative of Eq. 5a with respect to time must be zero and so:

$$\frac{\partial Z}{\partial t}(x_0(t),t)+\dot{x}_0(t)\frac{\partial Z}{\partial x}(x_0(t),t) = 0 \tag{5b}$$

with $\dot{x}_0 = dx_0/dt$. One may consider now the dynamic equilibrium of a piece of riser, placed on the right of $x_0(t)$ and with a suspended length $\Delta x(t)$ (Fig. 2).

If $\boldsymbol{F}(t)$ is the impact force between the riser and soil, Newton's equation in the vertical direction can be written in the form:

$$\frac{d}{dt}\left[(m+m_a)\Delta x(t)\frac{\partial Z}{\partial t}\right] = \boldsymbol{F}(t)+T_0\frac{\partial Z}{\partial x}(x_0+\Delta x,t)-q\Delta x(t)$$

if the dynamic tension $\tau(t)$ is disregarded when compared with T_0. Observing that $d\Delta x(t)/dt = -\dot{x}_0(t)$, taking the limit of the above expression when $\Delta x(t) \to 0$ and using Eq. 5b, one gets, with the help of Eq. 4:

$$\left[\dot{x}_0^2(t)-c_0^2\right](m+m_a)\frac{\partial Z}{\partial x}(x_0(t),t) = \boldsymbol{F}(t) \tag{5c}$$

The geometric constraint given by the soil imposes $Z(x,t) \geq 0$ and since $Z(x_0(t),t) = 0$, one must have $\partial Z/\partial x \geq 0$ at $x = x_0(t)$; at the same time, the contact between the riser and the rigid foundation is of the unilateral type and so $\boldsymbol{F}(t) \geq 0$. It follows, from Eq. 5c, that both the contact force $\boldsymbol{F}(t)$ and the angle $\partial Z/\partial x$ must be zero at the touchdown point when $\dot{x}_0 < c_0$; if $\dot{x}_0 > c_0$ then one can have an impact ($\boldsymbol{F}(t) > 0$), in which case the angle between the soil and riser is positive at the touchdown. The physical explanation of this result is simple to understand if one recalls that c_0 is the wave velocity in the vicinity of O: When $\dot{x}_0 < c_0$, the horizontal velocity of the touchdown point is smaller than the wave velocity, and the cable has enough time to adjust its geometric configuration and it runs smoothly on the ground; when $\dot{x}_0 > c_0$, the velocity of the touchdown point is greater than the wave velocity, and the cable has no time to adjust its configuration to the new touchdown position. In this case the riser strikes the soil, a phenomenon indeed very similar to the shock phenomenon in gas dynamics, and the asymptotic result to be developed in the paper is not valid.

The shock condition $\dot{x}_0 > c_0$ is rare and should not be expected in the present problem; as a matter of fact, one usually has $\dot{x}_0 << c_0$ in the situations to be analyzed, as discussed in the next item and confirmed by the numerical results shown. It follows, in this case, that the cable satisfies, at the touchdown point, the boundary condition:

$$\frac{\partial Z}{\partial x}(x_0(t),t) = 0 \tag{5d}$$

in accordance with Eq. 3b; see also Eqs. 3a and 5a.

If Eq. 5d is placed in Eq. 5b, one obtains:

$$\frac{\partial Z}{\partial t}(x_0(t),t) = 0 \tag{6a}$$

meaning that the vertical velocity at the touchdown point is always zero if there is no impact phenomenon. The vertical acceleration, however, is different from zero: If one derives Eqs. 5d and 6a with respect to time, in the manner indicated in Eq. 5b, one obtains:

$$\frac{\partial^2 Z}{\partial t^2}(x_0(t),t) = \dot{x}_0^2\frac{\partial^2 Z}{\partial x^2}(x_0(t),t) \tag{6b}$$

Eqs. 6a and b will be used in the analysis of the dynamic curvature at the touchdown point, but it is worthwhile, before one leaves this section, to make a digression that can place these results in a more enlightened perspective.

In fact, if one recalls that $\partial^2 Z/\partial x^2 = 1/R_c(t)$, where $R_c(t)$ is the instantaneous radius of curvature, one can imagine a circular cylinder with radius $R_c(t)$ rolling, without slipping, on the rigid flat bottom with a horizontal velocity $\dot{x}_0$ (Fig. 2). In this case, as is known, the vertical velocity at the cylinder's touchdown point is zero, as in Eq. 6a, while the acceleration is equal to $\dot{x}_0^2/R_c(t)$, as in Eq. 6b. Thus the cable can be locally attached to this cylinder, with a radius equal to the instantaneous cable's radius of curvature, and will roll smoothly on the ground with it when $\dot{x}_0/c_0 < 1$; this observation may make it easier to visualize the dynamic motion of the cable in the vicinity of its touchdown point.

Linear Dynamic Problem and Estimation of $x_0(t)$

The typical length scale in the touchdown region is the catenary radius of curvature $R_c = T_0/q$ and a simple analysis can indicate the order of magnitude of this value. In fact, since the static moment is of order EJ/R_c (Eq. 1b), the static deformation is given by $D/2R_c$, where D is the riser's outer diameter. Observing that the steel's yield strain is of order 1/500 and assuming a static stress below 25% of the yield stress, one must have $R_c > 1000\ D$; for a small-diameter steel riser one has $D \cong 8"$ and so $R_c > 200$ m. The imposed motion at the suspended end B has an amplitude of order $A_B \cong 3$ m for the extreme wave condition and one should expect a displacement $x_0(t)$ of the touchdown point not very much larger than this value; it turns out then that, in general, one must have $x_0(t) << R_c$, a condition that indicates that the dynamic problem can be linearized, as discussed below.

In fact, from Taylor's series expansion around the origin O, one gets:

$$Z(x_0(t),t) = Z(0,t)+x_0(t)\frac{\partial Z}{\partial x}(0,t)+O\left(x_0^2(t)\right) \equiv 0$$

$$\frac{\partial Z}{\partial x}(x_0(t),t) = \frac{\partial Z}{\partial x}(0,t)+x_0(t)\frac{\partial^2 Z}{\partial x^2}(0,t)+O\left(x_0^2(t)\right) \equiv 0$$

If the second identity is multiplied by $x_0(t)$ and subtracted from the first, one obtains that $Z(0,t)$ is of order $x_0^2(t)/R_c$. Neglecting dynamic quadratic terms, the following condition can be derived at the *static* touchdown point O for the *dynamic* solution:

$$Z(0,t) = 0 \tag{7a}$$

It follows that the *static* touchdown point is *vertically hinged* in the *linear dynamic* problem, although a horizontal spring (with stiffness $R = EA/L_E$, $L_E = T_0/\mu q$) must be placed there to accommodate the elastic deformation of the cable on the soil. With these linear boundary conditions the dynamic problem can be solved in the frequency domain. One should observe, however, that the angle $\partial Z/\partial x$ is not zero at O, a fact that allows one to determine the displacement $x_0(t)$ of the touchdown point. Indeed, from the second Taylor expansion shown above one gets:

$$x_0(t) = -\frac{T_0}{q}\frac{\partial Z}{\partial x}(0,t) = -\frac{T_0}{q}\alpha(0,t) \tag{7b}$$

if second order dynamic terms are neglected again and $\alpha(0,t) = \partial Z/\partial x$ designates the dynamic angle at O.

The angle $\alpha(0,t)$ can be determined from the linear frequency domain solution and the displacement $x_0(t)$ of the touchdown point can be estimated by Eq. 7b. To visualize the typical order of magnitude of the parameters x_0/R_c and $\dot{x}_0/c_0$ one must obtain first a rough estimation of the angle $\alpha_0(t) = \alpha(0,t)$ and of the wave velocity c_0, as is done in the following.

Suppose that A_B is the amplitude of the motion imposed in B and θ_B is the angle between the tangent to the catenary in B and the horizontal; $\theta_m = \theta_B/2$ is the "average" angle that the "cable" makes with the segment OB. Ignoring any possible dynamic effect, the displacement of B, in the direction of OB by an amount A_B, diminishes the angle θ_m by a value $\alpha_0 \approx (3/\theta_m)\, A_B/l$, if the "cable" is assumed inextensible and the angle is "small"; taking also $\theta_m \approx ql/2T_0$ and denoting by X_0 the amplitude of the touchdown displacement, the following relation can be obtained:

$$\frac{X_0}{A_B} \approx \frac{6}{\theta_B^2} \tag{8a}$$

Obviously, the above result gives only a rough estimate of the touchdown displacement, since it does not consider any dynamic effect and assumes also a "small" angle θ_m; it shows, however, that X_0/A_B increases as θ_B decreases, a conclusion that seems reasonable. Also, from Eq. 7b, one obtains that $X_0/R_c = \alpha_0 \approx (3/\theta_m)\, A_B/l << 1$ in deep water; this is the reason, it is believed, why the linear frequency domain solution predicts with reasonable accuracy the cable's dynamic response, even in an extreme wave condition; see, for instance, the results presented below.

To estimate the parameter $\dot{x}_0/c_0$ one must first determine a convenient expression for the wave velocity c_0. Assuming, for this purpose, that the ocean current $V(z)$ is zero, one has, from an equilibrium consideration, that $T_0 = T_B \cos\theta_B$ and $ql = T_B \sin\theta_B$, with θ_B being the angle in B. Since $q = (m - m_a)g$, using the definition of the wave velocity, one gets:

$$\left|\frac{\dot{x}_0}{c_0}\right|^2 = \left(\frac{m+m_a}{m-m_a}\right)\tan\theta_B \frac{\omega^2 A_B}{g}\frac{A_B}{l}\left|\frac{X_0}{A_B}\right|^2 \tag{8b}$$

A steel catenary riser is to be anchored in a deep-water floating production system, like a semisubmersible, for example, that responds weakly to the wave action. In this case one has that $\omega^2 A_B/g$ is smaller than $KA << 1$, with KA being the wave steepness, and certainly $A_B/l << 1$ in deep water. It happens then that one should have $\dot{x}_0/c_0 << 1$, as anticipated above.

Dynamic Tension $\tau(t)$

The dynamic tension $\tau(s,t)$ is the most important dynamic parameter of the cable. In the usual range of wave frequencies ω the elastic axial modes are not excited and the dynamic tension is essentially constant along the suspended length, as discussed in Triantafyllou et al. (1985), for example. One may take then $\tau(s,t) \cong \tau(t)$ in a "large" vicinity of O, with:

$$\tau(t) = \tau_1 \cos\omega t \tag{9}$$

The tension amplitude τ_1 can be determined directly from a linear frequency domain model, as discussed in the last item, although in this case one may consider the *global* dynamic equilibrium of the suspended cable to obtain a simple algebraic approximation, as shown in Aranha et al. (1993); this latter approach will be not discussed here although the results obtained from it will be used for the sake of comparison.

It is important to point out also that the computed tension values, both from this algebraic expression and the linear frequency domain solution, agree well with experimental results even in a extreme condition (Andrade, 1995). This result confirms the linear model assumption adopted in the present work.

Cable's Curvature in Vicinity of Touchdown Point

One turns now to the main topic of this work, the dynamic curvature in the touchdown region. Observing that the normal to the cable is essentially vertical in this region, while the ocean current is horizontal, the effect of this environmental load can be locally disregarded in the vicinity of O. Using again the approximation $x \cong s$ and denoting by $F_z(x,t)$ the vertical force, the dynamic equilibrium in this direction, including the fluid drag effect, is expressed by the equation:

$$\frac{\partial F_z}{\partial s}(x,t) = q+(m+m_a)\frac{\partial^2 Z}{\partial t^2}(x,t)+\frac{1}{2}\rho C_D D\left|\frac{\partial Z}{\partial t}(x,t)\right|\frac{\partial Z}{\partial t}(x,t)$$

Using Eqs. 6a and b in the above equality, one obtains:

$$\frac{\partial F_z}{\partial s}(x_0(t),t) = q+(m+m_a)\dot{x}_0^2(t)\frac{\partial^2 Z}{\partial x^2}(x_0(t),t)$$

and if cubic dynamic terms are neglected ($\partial^2 Z/\partial x^2 \cong q/T_0$) the following result can be derived:

$$\frac{\partial F_z}{\partial s} = q\left[1+\left(\frac{\dot{x}_0}{c_0}\right)^2\right];\ x \approx x_0(t) \tag{10a}$$

Let $\Theta(s,t) = \theta(s) + \alpha(s,t)$ be the total angle, $T(s,t)$ the total tension and $F_x(s,t)$ the horizontal force; by definition one has:

$$T(s,t) = F_x(s,t)\cos\Theta(s,t)+F_z(s,t)\sin\Theta(s,t)$$

while the shear force is given by:

$$Q(s,t) = F_x(s,t)\sin\Theta(s,t)-F_z(s,t)\cos\Theta(s,t) \equiv 0$$

Deriving the above identity with respect to s, noticing that $\Theta(s,t) \cong 0$ in the vicinity of the touchdown point and using Eq. 10a, one obtains:

$$T(s,t)\frac{\partial\Theta}{\partial s} = q\left[1+\left(\frac{\dot{x}_0}{c_0}\right)^2\right] \tag{10b}$$

Taking into account that:

$$T(s,t) = T_0+\tau(t) \tag{10c}$$

$$\frac{\partial\Theta}{\partial s}(s,t) = \chi(t) \tag{10d}$$

where $\chi(t)$ is the *total* dynamic curvature, the following expression can be derived in the vicinity of the touchdown point:

$$(T_0+\tau(t))\cdot\chi(t) = q\cdot\left[1+(\dot{x}_0/c_0)^2\right] \tag{10e}$$

Ignoring the dynamic quadratic term $(\dot{x}_0/c_0)^2$ and observing that the *total* moment (static plus dynamic) $M(t)$ is equal to $EJ.\chi(t)$, the result below can be obtained with the help of Eq. 1b:

$$M(t) = \frac{M_0}{1+\tau(t)/T_0}; \quad x \geq x_0(t) \tag{10f}$$

This expression is exact for the cable when the *local* inertia force, related to the parcel $(\dot{x}_0/c_0)^2$, is neglected.

Local Effect of Flexural Stiffness on Dynamic Moment

In the vicinity of the touchdown point the total curvature $\chi(t)$ is given by $\partial^2 Z/\partial x^2$, where $z = Z(x,t)$ represents, as before, the cable's dynamic configuration in the region. Using this notation in Eq. 10b and ignoring second order terms (Eqs. 10c and d), one obtains:

$$-(T_0+\tau(t))\frac{\partial^2 Z}{\partial x^2} = -q; \quad x \geq x_0(t) \tag{11a}$$

that is exactly the linearized *static* equation of a cable with weight q subjected to the *static* tension $(T_0 + \tau(t))$; observing that $M(t) = EJ\partial^2 Z/\partial x^2$ and recalling Eq. 1b, the above expression coincides, as it should, with Eq. 10f. If the flexural stiffness is included in the analysis, one obtains, in accordance, the equation:

$$EJ\frac{\partial^4 Z_f}{\partial x^4}-(T_0+\tau(t))\frac{\partial^2 Z_f}{\partial x^2} = -q; \quad x \geq x_f(t) \tag{11b}$$

with $x_f(t)$ being the instantaneous touchdown point when the flexural stiffness is incorporated.

This equation is similar to the one previously solved for the static problem and the final result can be obtained by inspection. In fact, the *flexural length* is now given by $\hat{\lambda} = \lambda(1+\tau(t)/T_0)^{-1/2}$ and the flexural stiffness displaces the *instantaneous* cable's touchdown point to the left by an amount $-\hat{\lambda}$, which leads to $x_f(t) = x_0(t) - \hat{\lambda}$; introducing the variable:

$$\beta(s,t) = \frac{\sqrt{1+\tau(t)/T_0}}{\lambda}\cdot\left[s-x_0(t)+\frac{\lambda}{\sqrt{1+\tau(t)/T_0}}\right] \tag{12a}$$

the dynamic moment in the touchdown region can be written as:

$$M_f(s,t) = \frac{1}{2}(1+sign\beta(s,t))\left[1-e^{-\beta(s,t)}\right]\frac{M_0}{1+\tau(t)/T_0} \tag{12b}$$

The solution given by Eq. 12, based on a local correction of the cable's Eq. 11a, does have meaning only when $\tau(t)/T_0 < 1$ since, otherwise, the cable becomes statically unstable and cannot be used as a basis for the riser's solution.

In the fatigue analysis one is interested in the cyclic variation of the bending moment caused by a low sea state, where $\tau(t)/T_0 << 1$; if this parcel is disregarded in the last term of Eq. 12b and:

$$x_0(t) = X_0\cos(\omega t+\psi) \tag{13a}$$

with X_0 being the amplitude of the cable's touchdown displacement, then the point in the riser where the range ΔM of the oscillatory moment is maximum is defined by the expression:

$$\left(\frac{s}{\lambda}\right)_{MAX} = -1+\frac{X_0}{\lambda} \tag{13b}$$

while ΔM is approximately given by:

$$(\Delta M)_{MAX} = \left(1-e^{-2X_0/\lambda}M_0\right) \tag{13c}$$

This result shows that the fatigue analysis depends essentially on the static curvature q/T_0 of the catenary and on the ratio between the amplitude X_0 of the touchdown displacement and the *flexural length* λ. It follows, also, that mathematical models that do not consider the running of the touchdown point should, in general, underestimate ΔM. At the same time, a local increase in EJ, in the vicinity of point O in Fig. 1, can have a beneficial effect since it increases locally the flexural length λ.

NUMERICAL RESULTS

In order to check the analytical approximation given by Eq. 12, 2 risers have been analyzed, one with an external diameter of 16" to export oil, and the other with diameter of 8 5/8" to export gas. The 2 risers are assumed to have a global length of 5000 m, the soil is supposed to be rigid, the friction coefficient μ to be equal to 0.4 and the drag coefficient $C_D = 1.1$; the relevant mechanical properties and static parameters of these risers appear in Table 1.

Nine distinct sea states in Campos Basin were considered in the fatigue analysis and an extreme (centenary) condition was also analyzed for the 16" riser; in all cases the ocean current was

	RISER 16"	RISER 8 5/8"
h	575 m	910 m
D	0.4064 m	0.2191 m
q	1.19 kN/m	0.26 kN/m
EJ	78000 kN m^2	9241 kN m^2
EA	$4x10^6$ kN	$2x10^6$ kN
xB	784 m	733 m
zB	590 m	900 m

Table 1 Mechanical and static riser's parameters

SEA	PERIOD	A_B
1	7.08 s	0.07 m
2	7.11 s	0.12 m
3	7.74 s	0.20 m
4	8.41 s	0.32 m
5	9.23 s	0.47 m
6	10.16 s	0.70 m
7	10.33 s	0.84 m
8	10.64 s	1.02 m
9	11.41 s	1.31 m
EXT	12.04 s	2.20 m

Table 2 Period and amplitude of harmonic circular motion for different sea states

assumed to be zero. For a more direct comparison between the analytical approximation and the numerical results, for each sea state an equivalent circular motion, with amplitude A_B and period P, was assumed (Table 2).

A homemade program, RISDIN, was developed to analyze the "cable" (EJ = 0) in the frequency domain, as explained before, and two commercial softwares, SOFT-1 ("ORCAFLEX" in Larsen, 1992) and SOFT-2, were also run in the study. These programs use a nonlinear time domain model with lumped masses and only SOFT-1 was used in the extreme situation (16" riser).

The SOFT-2 is a software whose technical accuracy is not published in the literature.

Table 3 compares, for the 16" riser, the rms value of the dynamic tension determined by the software with the values obtained from RISDIN and also by the algebraic expression derived in Aranha et al. (1993), named ASYMPT here; notice that $\tau_1 = \sqrt{2}$ rms $\tau(t)$. The two last columns present the relevant parameters of the touchdown motion. In Table 4 the same comparison is made with respect to the 8 5/8" riser. All cases here refer to an imposed circular motion in the *counter-clockwise direction* and this is an important, although unexpected, feature: As will be seen below, the displacement of the touchdown point, and thus the dynamic moment, are sometimes very sensitive to the sense of rotation imposed at the suspended end (mainly for the 16" riser in the three first sea states). Since the quasi-linear frequency domain cable's model captures this feature very well (see Figs. 3 and 4) and the only nonlinear aspect of this model is the fluid drag, the observed sensibility with respect to the sense of rotation is due to this parcel; indeed, when the damping factor is truly linear no difference has been observed with respect to the sense of rotation.

For the 16" riser the static tension is T_0 = 714 kN at the static touchdown point and the flexural length is then λ = 10.4 m. A first observation should be made about the results presented in Tables 3 and 4: Both the algebraic approximation ASYMPT and the linear frequency domain model RISDIN predict, with reason-

SEA	ASYMPT	RISDIN	SOFT-1	SOFT-2	$\dot{x}_0/c_0$	X_0/A_B
1	14.4	12.6	11.9	10.5	0.04	29.9
2	24.5	22.0	18.9	18.6	0.06	24.1
3	33.8	31.9	30.2	29.3	0.09	21.4
4	45.2	46.4	43.0	37.0	0.10	17.4
5	55.1	57.3	55.0	43.6	0.09	12.8
6	69.2	73.2	73.0	59.8	0.12	12.6
7	82.6	89.0	88.9	72.8	0.16	13.0
8	98.1	111.1	108.0	90.0	0.19	13.2
9	116.8	133.2	132.5	117.9	0.22	13.2
EXT	223.5	266.8	253.3	*	0.38	14.3

Table 3 Rms of dynamic tension (kN) for 16" riser, counterclockwise motion; values from algebraic expression, ASYMP, from linear frequency domain, RISDIN, and from nonlinear time domain models, SOFT-1 and SOFT-2. Also shown, velocity and amplitude of touchdown displacement.

SEA	ASYMPT	RISDIN	SOFT-1	SOFT-2	$\dot{x}_0/c_0$	X_0/A_B
1	2.2	1.6	1.9	1.5	0.01	11.6
2	3.7	3.2	3.5	2.6	0.03	12.1
3	5.2	5.0	5.1	4.0	0.05	13.8
4	7.3	7.4	7.4	5.4	0.06	11.9
5	9.3	9.9	9.9	7.2	0.08	11.2
6	12.6	14.3	13.9	11.1	0.11	11.2
7	15.6	18.2	17.3	14.5	0.16	11.5
8	19.5	23.4	21.8	18.9	0.16	11.8
9	25.0	31.2	28.4	27.3	0.19	12.0

Table 4 Rms of dynamic tension (kN) for 8 5/8" riser, counterclockwise motion; values from algebraic expression, ASYMP, from linear frequency domain, RISDIN, and from nonlinear time domain models, SOFT-1 and SOFT-2. Also shown, velocity and amplitude of touchdown displacement.

ably good precision, the dynamic tension even in the extreme condition, when $\tau_1 \approx T_0/2$ and a strong nonlinear effect is expected. The same conclusion holds true for the 8 5/8" riser.

In both cases the amplitude X_0 of the touchdown displacement, computed from Eq. 7b, is roughly 4 times the estimate given by Eq. 8a; this result, however, does not invalidate the order of magnitude analysis presented then. The *local inertia parameter* $(\dot{x}_0/c_0)^2$ is of the order 14% for the centenary sea state and very small for the remaining ones.

The behavior of the moment can be better visualized in graphical form and, for this reason, only some results will be displayed here. Attention will be focused then on the 16" riser subjected to sea state 3, the most likely one in Campos Basin, and to the extreme environmental condition. The results, however, are typical and illustrate the main features of the dynamic moment.

For sea state 3 the oscillatory moment has been characterized by its average and rms values. Both parameters were plotted, in Figs. 3 and 4, against s/λ, with s = 0 at O, namely, at the static touchdown point of the cable (EJ = 0). In Fig. 5 the relevant parameter in the fatigue analysis, namely, the peak-to-peak value of the moment in one point, was plotted as a function of s/λ.

Figs. 3~5 show the comparison between the analytical approximation and numerical results obtained from SOFT-1 when the suspended end rotates in the *clockwise* and *counter-clockwise* directions. The agreement between the analytical and numerical results is very good and both the quasi-linear frequency domain and the full nonlinear time domain models show the enormous

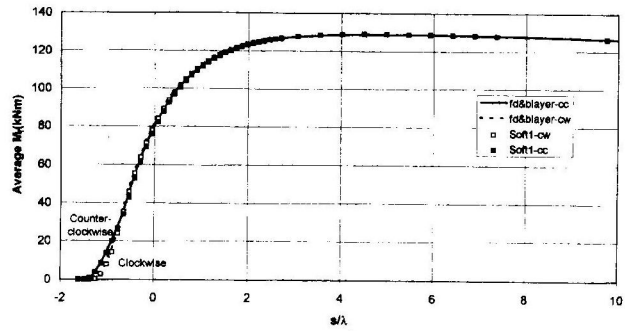

Fig. 3 Average value of moment in vicinity of touchdown point. Sea state 3, 16" riser. fd: frequency domain; blayer: boundary-layer solution; SOFT1: time-domain simulation program 1; cc: counterclockwise; cw: clockwise.

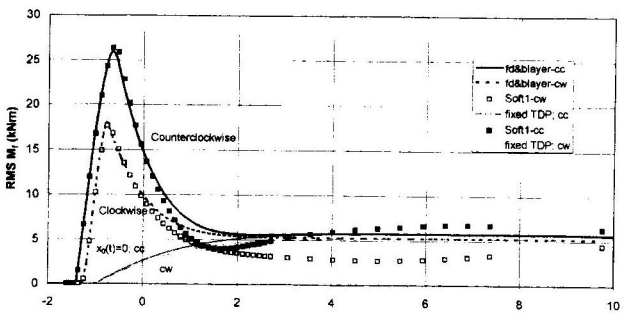

Fig. 4 RMS value of moment in vicinity of touchdown point. Sea state 3, 16" riser. fd: frequency domain; blayer: boundary-layer solution; SOFT1: time-domain simulation program 1; cc: counterclockwise; cw: clockwise.; $x_0(t) \equiv 0$: TDP not allowed to move.

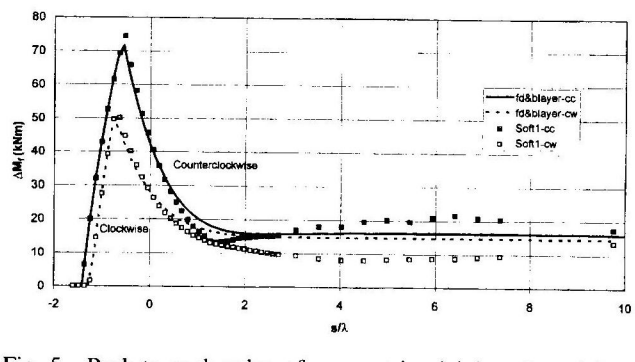

Fig. 5 Peak-to-peak value of moment in vicinity of touchdown point. Sea state 3, 16" riser. fd: frequency domain; blayer: boundary-layer solution; SOFT1: time-domain simulation program 1; cc: counterclockwise; cw: clockwise.

difference (almost a factor two) in the rms of the moment, depending on the sense of the imposed rotation at the suspended end. This is obviously a nonlinear effect that, being captured by the quasi-linear frequency domain model, can be caused only by the viscous drag; in fact, when the damping is assumed to be truly linear (as in the presence of a strong ocean current), no difference has been observed with respect to the sense of rotation. Actually, the sense of rotation affects weakly the average value of the bending moment (see Fig. 3) and the dynamic tension $\tau(t)$, but it influences strongly the displacement $x_0(t)$ of the touchdown point: When the suspended end rotates in a counterclockwise direction, the amplitude of the touchdown displacement is 1.8 times greater than when the rotation is clockwise; if one uses the approximation $e^{-2X_0/\lambda} \approx 1-2X_0/\lambda$ in Eq. 13, it follows that the ratio between $(\Delta M)_{MAX}$ in the two cases is roughly of the order of the ratio between X_0, a conclusion confirmed by the results shown in Fig. 5.

In the time domain simulation a mesh with Δs = 1.25 m was used in the vicinity of O, to follow the bending moment variation; to ensure numerical stability with this mesh size, the time step had to be taken $\Delta t = 12\times10^{-6}$ s. On the other hand, to settle down the transient motion, the dynamics had to be simulated during a real time as long as 60 s, since the riser's natural period is around 20 s in the case. These numbers give an idea of the amount of numerical work needed when the scales are too discrepant.

For sea state 3 the amplitude X_0 of the touchdown displacement, when the suspended end rotates in the *counterclockwise* direction, is equal to 4.3 m (Tables 2 and 3), and so $X_0/\lambda = 0.41$. For this case the simplified Eq. 13 predicts that the maximum peak-to-peak value ΔM will happen at $(s/\lambda)_{MAX} = -0.59$ and it will be given by $(\Delta M)_{MAX} \cong 73$ kNm, in very close agreement with both the numerical results and the full expression (Eq. 12, Fig. 5). It follows that Eq. 13 can be used in a first estimate for the fatigue life of a riser. One must observe, however, that the point where ΔM is maximum changes with X_0, and so with the sea state, and it may be too conservative to assume that the maximum of ΔM holds at the same point for all sea states.

The observed pronounced maximum value of rms $M(t)$ or ΔM is directly related to the motion of the touchdown point. In fact, when this moves, there are points in the riser that are cyclically "laid down" and "lifted off," causing a cyclic variation of the moment between zero and (roughly) the static value, a variation in general much greater than in other parts of the riser. Enlightening this argument, Eq. 12, with $x_0(t) \equiv 0$, is also plotted in Fig. 4; in this situation no points in the riser can be lifted off or laid down and the peak value of rms $M(t)$ disappears. Mathematical models that do not take into full account the touchdown motion can then grossly underestimate the cyclic variation of the moment, which is crucial in the fatigue analysis; *notice that the small horizontal motion allowed to accommodate the elastic deformation of the part of the riser on the ground, is far from enough to cope with the real touchdown motion.*

For the extreme sea condition, one is interested in the maximum value of the moment and Fig. 6 displays this value as computed from Eq. 12 and SOFT-1. In this case the nonlinearity is strong, since $\dot{x}_0/c_0 \cong 0.38$ (Table 3), and the expected error of the

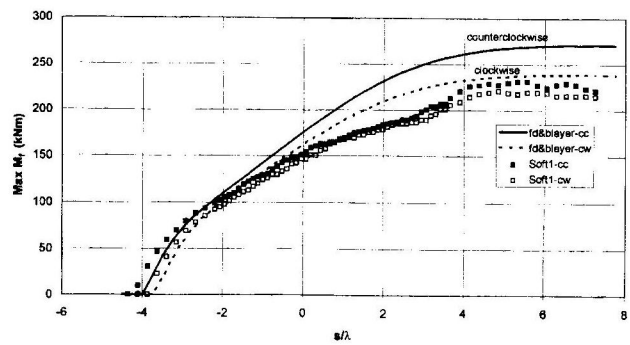

Fig. 6 Maximum value of moment. Extreme sea state, 16" riser. fd: frequency domain; blayer: boundary-layer solution; SOFT1: time-domain simulation program 1; cc: counterclockwise; cw: clockwise.

asymptotic approximation, where terms of order $(\dot{x}_0/c_0)^2$ are ignored, is of the order 15%, a value compatible with the one observed in Fig. 6.

CONCLUSION

In this paper, an asymptotic approximation of the boundary layer type was developed for the bending moment in the touchdown region of a riser, based on the quasi-linear frequency domain response of a cable ($EJ = 0$). If $x_0(t)$ is the displacement of the touchdown point (Eq. 7b), and $\tau(t)$ is the dynamic tension, the underlying assumptions in the present analysis are $\{\tau(t)/T_0 < 1;\ \dot{x}_0/c_0 < 1\}$, where T_0 is the static tension at the touchdown point and c_0 is the local wave velocity in the cable (Eq. 4). If $\tau(t)/T_0 > 1$, the cable buckles dynamically while a shock phenomenon is expected when $\dot{x}_0/c_0 > 1$. To be strict, neither one of these nonlinear phenomena should be observed for the actual riser, where the bending stiffness is non zero: On one hand, if $EJ \neq 0$ then certainly some compression in the line ($\tau(t)/T_0 > 1$) is allowed; on the other hand, under the same condition $EJ \neq 0$ the waves become dispersive and one should expect, when $\dot{x}_0/c_0 > 1$, a competing mechanism between dispersion and nonlinearity (Whitham, 1974), leading eventually to a solitary wave behavior and not to a shock wave. In any case the conditions $\{\tau(t)/T_0 > 1;\ \dot{x}_0/c_0 > 1\}$ should be avoided, since otherwise the loads would be so large as to impair the use of the steel catenary solution; in reality, the underlying assumptions $\{\tau(t)/T_0 < 1;\ \dot{x}_0/c_0 < 1\}$ are usually fulfilled in an actual problem, as shown by the examples discussed in this paper.

For all sea states used in the fatigue analysis, the derived expression, Eq. 12, compares very well with numerical results obtained from nonlinear time domain models and the comparison is good even for the extreme (centenary) sea state in Campos Basin.

Besides being much more efficient than the time domain solution, the derived expression, being analytical, can also be used as a theoretical tool to study some features of the bending moment in the touchdown region. In this respect one should call attention to the simplified Eq. 13, which can be important in the riser's design, and to the possibility of analyzing the statistical behavior of the dynamic tension (bending moment) in a relatively easy way: In fact, Eq. 12 shows that the bending moment, although strongly nonlinear, depends only on two dynamic variables of the cable, namely, the dynamic tension $\tau(t)$ and the touchdown displacement $x_0(t)$. Since these variables are quasi-linear (as a matter of fact, they become essentially linear when the ocean current is strong and the fluid drag can be linearized), Eq. 12 can be used to study the complex nonlinear statistics of the bending moment using time series realizations of the quasi-linear variables $\{\tau(t); x_0(t)\}$.

ACKNOWLEDGEMENTS

This work has been partially supported by PETROBRÁS. The authors also acknowledge a grant from CNPq and useful discussions with MEng MMO Pinto, MEng B.L.R. Andrade and Dr. A.C. Fernandes.

REFERENCES

Andrade, BLR (1995). "Mooring Lines Dynamics: an Experimental Study and a Frequency Domain Calculation Method," *MSc Thesis,* Dept Naval and Ocean Eng, Univ São Paulo (in Portuguese).

Aranha, JAP, Pesce, CP, Martins, CA, and Rodrigues, BLA (1993). "Mechanics of Submerged Cables: Asymptotic Solution and Dynamic Tension," *Proc 3rd Int Offshore and Polar Eng Conf,* Singapore, ISOPE, Vol II, pp 345-356.

Burridge, R, Kappraff, J, and Morshedi, C (1982). "The Sitar String: A Vibrating String with a One-Sided Inelastic Constraint," *SIAM J Applied Math,* Vol 42, No 6, pp 1231-1251.

Larsen, CM (1992). "Flexible Riser Analysis — Comparison of Results from Computer Programs," *Marine Struct,* Vol 5, No 5, pp 103-119.

Phifer, EH, Kopp, F, Swanson, RC, Allen, DW, and Langner, CG (1994). "Design and Installation of Auger Steel Catenary Riser," *Proc Offshore Tech Conf,* Houston, pp 399-408.

Triantafyllou, MS, Bliek, A, and Shin, H (1985). "Dynamic Analysis as a Tool for Open Sea Mooring System Design," *Ann Meeting Soc Naval Arch and Marine Eng,* New York.

Whitham, GB, (1974). *Linear and Non-linear Waves,* Pure and Applied Mathematics, Wiley-Interscience Series of Texts, Monographs and Tracts, 636 pp.